

© Copyright 2001 IEEE. IEEE Semiannual Vehicular Technology Conference (VTC2001 Spring), May 6 -9, 2001, Rhodes, Greece

Personal use of this material is permitted. However, permission to reprint/republish this material for advertising or promotional purposes or for creating new collective works for resale or redistribution to servers or lists, or to reuse any copyrighted component of this work in other works must be obtained from the IEEE.

Measurement of the capacity of MIMO systems in frequency-selective channels

A. F. Molisch
AT&T Labs-Research
200 Laurel Av.

Middletown, NJ, USA
Andreas.Molisch@tuwien.ac.at
formerly INTHF, TU Wien

M. Steinbauer, M. Toeltsch, E. Bonek
INTHF
TU Wien

Gusshausstrasse 25/389
Vienna, Austria

R. S. Thoma
IKM
TU Ilmenau
Ilmenau, Germany

Abstract

We analyze the capacity of multiple-input - multiple-output (MIMO) systems in microcellular environments, taking into account the frequency selectivity of the wireless channels. We use a new data evaluation method that allows to evaluate the probability density function (pdf) of the capacity from a single measurement. We find that the frequency selectivity of the channel makes the pdf more peaked, and thus increases the outage capacity compared to the frequency-flat case. However, capacities are considerably lower than predicted for ideally decorrelated channels.

1 Introduction

In recent years, the interest in multiple-input - multiple-output (MIMO) systems, i.e., systems with multiple antennas at both transmitter and receiver, has exploded. As the transmission paths via the different scatterers provide independent communications channels, large capacities can be achieved. It was shown that with M antennas at both transmitter and receiver, the channel capacity is increased by a factor M compared to the single-antenna case [23], [8], [2]. Space-time (ST) codes that come reasonably close to realizing this capacity have been proposed [21], [20], and commercial products based on those ideas are currently under development [5]. The earlier theoretical work assumed frequency-flat fading channels. Recently, interest has turned to the performance in frequency-selective channels, e.g. [4], [7]. There are two reasons for this interest: (i) MIMO systems are especially suitable for high-data-rate communications, which inherently cover larger bandwidths, and thus usually en-

counter frequency-selective channels (ii) the frequency diversity inherent in frequency-selective channels can be exploited to additionally increase the outage capacity of the system. The most practical approach for broadband-MIMO systems is MIMO-OFDM [12], [13], [1], [3], [14], but also single-carrier systems with equalizers or Rake-receivers can be used.

Most of the earlier theoretical work assumed ideal channels where the fading of the signals at all antenna elements was decorrelated. Recent investigations explored the effects of fading correlation and frequency selectivity by using more sophisticated channel models [17], [3], [9]. However, there is not substitute for real measurements - especially at the current state of research, where validation of the models is still required. In this paper, we report on a measurement campaign in a microcellular environment, and give results for the MIMO capacity in *frequency-selective* channels. Since wideband MIMO systems require a great deal of work and are thus expensive,¹ we introduce a method that allows to compute the probability density function of the capacity from a *single* measurement. We investigate the effects of bandwidth, SNR, and number of antennas.

2 Measurement setup and data evaluation

2.1 Measurement setup

Our double-directional measurements are performed with a RUSK ATM wideband channel sounder [22], operating at $5.2GHz$ (HIPERLAN II band). The channel sounder has a measurement bandwidth of $120MHz$. At

¹this is especially true for synthetic-aperture measurements

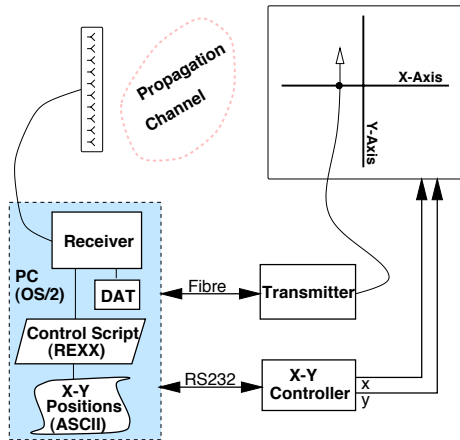


Figure 1. Setup of the double-directional measurements.

the transmitter, we use a virtual antenna array, i.e. a dipole antenna that is moved by a computer-controlled step-motor. The dipole was moved in a cross-shaped pattern in order to resolve the directions-of-arrival in an unambiguous way. At the receiver, we used a multiplexed array, i.e. a linear array of patch antennas that are connected to a fast RF switch, allowing to measure the impulse response of a different antenna element, e.g., every $100\mu\text{s}$. Because of the virtual array at the transmitter, measuring the transfer functions from all transmit to all receive antennas took several minutes. Thus, special care was taken to eliminate time variations of the channel during that time: on one hand, we performed 256 successive measurements, and performed low-pass filtering in the Doppler domain. On the other hand, we repeated measurements after about 10 minutes, and compared the results from the two measurements. The required synchronization was achieved by an optical fiber connection between transmitter and receiver, and a back-to-back calibration. More details about the measurement setup can be found in [19].

Measurements were performed in two courtyards in Ilmenau, Germany. In all cases, transmitter and receiver were at a height of about 1.5m . Two scenarios were line-of-sight, while the other two were non-LOS. Scenarios II and III were identical except for an intentional blocking of the LOS. Figures 1 and 2 show the layout of the measurement environments. The result of our measurements were three-dimensional transfer function matrices with dimensions (number of transmit antennas) \times (number of receive antennas) \times (number of frequency samples).

2.2 Data evaluation technique

As we will see below, our capacity evaluation technique is based on determining delays, directions-of-departure (DODs), and directions-of-arrival (DOAs) of the multipath components (MPCs). In order to extract those parameters from the transfer function matrices, we apply parameter estimation techniques, whose resolution is much better than Fourier techniques. Our method, explained in detail in [18], works the following way: we used a nested implementation of Unitary ESPRIT [10] which is an improved version of the classical ESPRIT algorithm [16]. Since we had to estimate parameters on three dimensions (delay, DOA, and DOD), we had to apply ESPRIT in a threefold-nested way.² The number of MPCs whose parameters can be estimated is limited by the number of samples in the respective dimension. Thus, it is advantageous to first estimate the delays, as we had 192 samples in the delay (or frequency) domain available. After estimation of the parameters τ_i , we can determine the corresponding “steering” matrix A_τ at each τ_i . Subsequent beamforming with its Moore-Penrose pseudoinverse [11] A_τ^+ gives the parametric 2-dimensional spatial vector channel impulse response $h(\tau_i, \vec{x}_T, \vec{x}_R)$:

$$h_{\tau_i}(\vec{x}_T, \vec{x}_R) = A_\tau^+ T_f(\vec{x}_T, \vec{x}_R). \quad (1)$$

This gives us now the two-dimensional transfer function from position \vec{x}_T to position \vec{x}_R separately for each delay τ_i . For each delay, we can now apply ESPRIT to find the DOA (where 8 samples are available), and finally for each DOA all possible DODs. This sequence of estimates thus allows to estimate a large number of MPCs.

We note, however, that the estimation of the total number of MPCs, which forms an important part of the ESPRIT algorithm, suffers from some ambiguities. While various criteria have been proposed in the literature, none can be considered “definite”. We found that the total power of the identified MPCs was lower than the total power as obtained from the measured transfer functions. This can be explained only in part by the noise in the system. A residual error due non-identified MPCs could not be eliminated.

3 Capacity computation

In a fading channel, the capacity is a random variable, i.e., depending on the local (or instantaneous) channel realization. In order to determine the cumulative distribution function (cdf) of the capacity, and

²In principle, it is also feasible to estimate the parameters jointly from one large matrix [6], [15].

thus the outage capacity, we would have to perform a large number of measurements either with slightly displaced arrays, or with temporally varying scatterer arrangement. Since each single measurement requires a huge effort, such a procedure is highly undesirable. To improve this situation, we use a new evaluation technique that requires only a *single* measurement of the channel. It is well-known that the phases of MPCs are uniformly -distributed random variables, whose different realizations occur as either transmitter, receiver, or scatterers move. We can thus generate different realizations of the transfer function from the k -th transmit to the m -th receive antenna by adding random phases to the MPCs, i.e.,

$$h_{k,m}(f) = \sum_i a_i \exp\left(j\frac{2\pi}{\lambda}dk \sin(\phi_{T,i})\right) \exp\left(j\frac{2\pi}{\lambda}dm \sin(\phi_{R,i})\right) \exp(j2\pi f\tau_i) \exp(j\alpha_i) \quad (2)$$

where α is a uniformly distributed random phase, who can take on different values for the different MPCs. Note, however, that α_i stays unchanged as we consider different antenna elements k and m .

Thus, we perform the following steps:

1. from a single measurement, determine the delays, DOAs, and DODs of the MPCs by nested application of ESPRIT.
2. compute synthetically the impulse responses at the positions of the antenna elements, and at different frequencies. Different realizations of one ensemble are created by Eq. 2.

The cdf of the channel capacity (for the case that the channel is unknown at the transmitter, i.e. no waterfilling is applied) is finally obtained by applying the capacity formula [8]

$$C = \int \log_2 \det \left[I_M + \frac{\gamma}{M} H^H(\omega) H(\omega) \right] d\omega \quad (3)$$

to each channel realization. Here, $H(\omega)$ is the frequency-dependent transfer matrix (dimension $M \times M$) with entries $h_{k,m}$, γ is the signal-to-noise ratio, I_M is the $M \times M$ identity matrix, and superscript H denotes Hermitian transposition. The integration range is the bandwidth of interest.

The accuracy of the "random phase" technique for the computation of the capacity can be assessed for the flat-fading channel. In this instance, we can compare the capacity cdf at the different measured frequencies (obtained directly from the transfer function measured by our channel sounder) to the capacity cdf as obtained

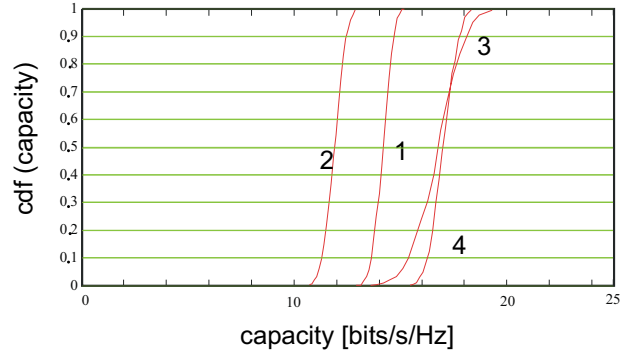


Figure 2. Capacity of the four measured scenarios with a 4×4 array at SNR=20dB. Narrow-band case.

by the random-phase technique for a flat-fading channel. We found that - due to the non-identified MPCs mentioned above - the 10 % outage capacities of the two methods differed by up to 1.5 bits/s/Hz in a 4×4 array with 20 dB SNR. The agreement was worst in non-LOS scenarios with a rich multipath structure, while for the LOS scenarios the main components could be identified very well, and thus the agreement between the two methods was better (deviation about 0.5 bit/s/Hz).

4 Results

Figure 2 shows the capacity of the four scenarios in our courtyards for *frequency-flat* channels and a 4×4 antenna array.³

Figure 3 shows the gain in mean capacity and outage capacity in Scenario 4 as we increase the bandwidth. Essentially, we would expect a gain in the outage capacity as we increase the bandwidth (note that we normalize the capacity to unit bandwidth in all cases). This should occur because the frequency selectivity of the channel adds additional diversity, so that the outage capacity becomes closer to the mean capacity. In scenario 4, the outage capacity improves from 16.2 *bits/s/Hz* to 17.1 *bits/s/Hz* when we increase the bandwidth from narrowband to 100MHz. This improvement is quite significant, but note that it requires a very large bandwidth. Wideband cellular and wireless LAN services use a bandwidth of 5 – 20 MHz, so that the improvement will be somewhat less in those cases. Specifically, the capacity in scenario 4 is 16.8 bits/s/Hz when the

³We see that the capacity of the LOS scenarios (1 and 2) is considerably smaller than for the NLOS scenarios. This is related to the fact that we have normalized to a fixed SNR, and not a fixed noise power.

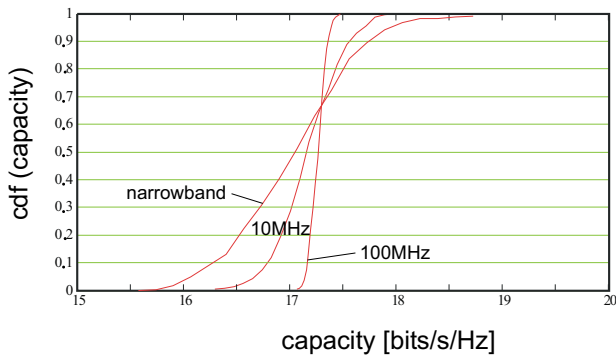


Figure 3. Capacity in scenario IV of a 4×4 array, SNR=20dB.

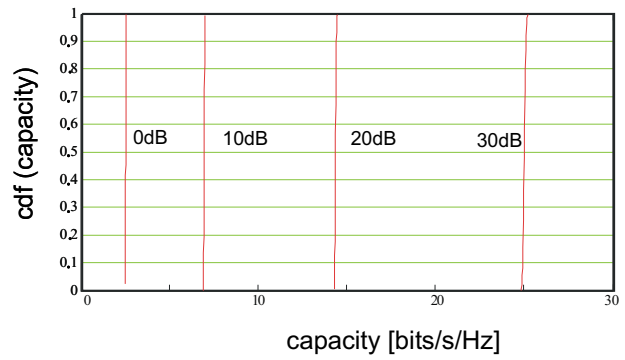


Figure 5. Capacity distribution for 100 MHz bandwidth and a 4×4 array in scenario II for various SNRs.

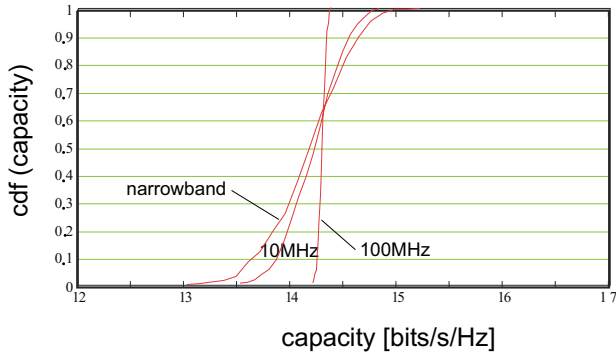


Figure 4. Capacity in scenario 2 for a 4×4 array, SNR=20dB.

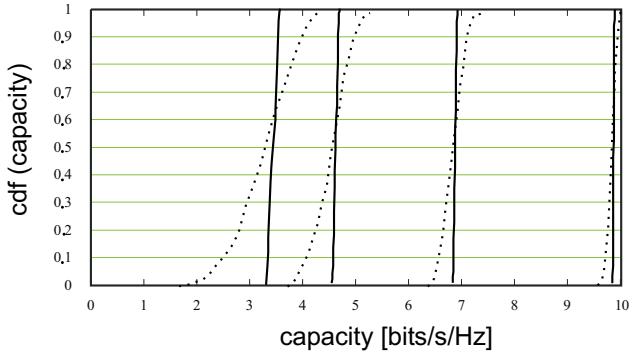


Figure 6. Capacity distribution for narrow-band (dotted) and 100 MHz bandwidth (solid) and 10 dB SNR in scenario II for array sizes $M = 1, 2, 4, 8$.

bandwidth is $10MHz$.⁴

Figure 4 shows the cdf of a LOS scenario, namely Scenario 2, which has a somewhat steeper cdf even in the narrowband case - a fact that is related to the existence of a LOS component. In this scenario, the 10% outage capacity increases from 13.6 bits/s/Hz via 13.9 bits/s/Hz to 14.2 bits/s/Hz.

Another interesting point is the improvement of the mean capacity by using wideband transmission in a frequency-selective channel. For the single-antenna case, it is well-known that the mean capacity is not improved by frequency diversity. However, reference [3] has shown theoretically that in MIMO systems, the frequency selectivity of the channel can increase also the mean capacity. Increases up to 30% were predicted for certain channel situations. However, in our measurements, we found only a small change in the mean

⁴Note again that we are talking here about improvements in the capacity normalized to unit bandwidth. Naturally, the total capacity of a 100 MHz system is about ten times as large as the total capacity of a 10 MHz system.

capacity as we increased the bandwidth and thus the frequency selectivity. Specifically, the increase was always less than 10%. This is probably due to the fact that the scatterer distribution in our scenarios differed appreciably from the one assumed in [3].

Next, we investigate the behavior of the narrowband and the wideband case for different SNRs. Figure 5 plots the cdf of the capacity for 0, 10, 20, and 30dB in a 4×4 array in scenario 2.

Finally, we investigate the improvement of the outage capacity by frequency diversity as a function of the array size. We find that both the relative and the absolute improvement decreases as the number of antennas increases, see Fig. 6. The reason for this behavior is that the additional antennas provide some degree of diversity, so that the additional diversity by the frequency diversity becomes less important.

5 Summary and conclusions

We have analyzed the capacity of MIMO systems in frequency-selective channels. In order to decrease the measurement effort, we have used a new technique that allows the computation of the complete cumulative distribution function of the capacity from a single measurement of the frequency-selective array transfer function. From this, we extracted the parameters (delay, DOA, and DOD of the multipath components). By adding up the MPCs with different (random) phase factors, we generated an ensemble of array transfer functions from this single measurement.

We then applied the technique to data collected in a measurement campaign in courtyards in Ilmenau, Germany. We found that the frequency selectivity of the channel significantly increases the outage capacity, but did hardly influence the mean capacity.

References

- [1] D. Agrawal, V. Tarokh, A. Naguib, and N. Seshadri. Space-time coded OFDM for high data-rate wireless communication over wideband channels. *VTC'98*, 3:2232–2236, 1998.
- [2] J. B. Andersen. Antenna arrays in mobile communications: gain, diversity, and channel capacity. *IEEE Antennas Propagation Mag.*, pages 12–16, April 2000.
- [3] H. Boelcskei, D. Gesbert, and A. J. Paulraj. On the capacity of OFDM-based multi-antenna systems. submitted 2000.
- [4] H. Boelcskei and A. J. Paulraj. Space-frequency coded broadband OFDM systems. In *IEEE WCNC*, IEEE, 2000.
- [5] H. Boelcskei, A. J. Paulraj, K. V. S. Hari, R. U. Nabar, and W. W. Lu. Fixed broadband wireless access: state of the art, challenges, and future directions. *IEEE Communications Mag.*, Jan. 2001.
- [6] E. Bonek and M. Steinbauer. Double-directional channel measurements. In *ICAP 2001*, in press, Manchester, 2001.
- [7] W. J. Choi and J. M. Cioffi. Space-time block codes over frequency selective Rayleigh fading channels. In *Proc. IEEE VTC 1999 - Fall*, pages 2541–2545, Amsterdam, 1999. IEEE.
- [8] G. J. Foschini and M. J. Gans. On limits of wireless communications in fading environments when using multiple antennas. *Wireless Personal Comm.*, 6:311–335, 1998.
- [9] D. Gesbert, H. Boelcskei, and A. Paulraj. Outdoor MIMO wireless channels: Models and performance prediction. *IEEE Trans. Comm.*, submitted, 2000.
- [10] M. Haardt and J. Nossek. Unitary ESPRIT: How to obtain increased estimation accuracy with a reduced computational burden. *IEEE Trans. on Signal Processing*, 43:1232–1242, 1995.
- [11] R. A. Horn and C. R. Johnson. *Matrix Analysis*. Cambridge Univ. Press, 1985.
- [12] Y. Li, N. Seshadri, and S. Ariyavisitakul. Channel estimation for OFDM systems with transmitter diversity in mobile wireless channels. *IEEE J. Selected Areas in Communications*, 17:461–471, 1999.
- [13] Y. G. Li, J. C. Chuang, and N. R. Sollenberger. Transmitter diversity for OFDM systems and its impact on high-rate data wireless networks. *IEEE J. Selected Areas Comm.*, 17:1233–1243, 1999.
- [14] A. F. Molisch, M. Z. Win, and J. H. Winters. Space-time-frequency-coding for MIMO-OFDM systems. *Proc. 4th European Personal Mobile Comm. Conf.*, 2001.
- [15] A. G. Richter, D. Hampicke, G. Sommerkorn, and R. Thoma. Joint estimation of DoD, time-delay, and DoA for high-resolution channel sounding. *Proc. IEEE VTC2000 -Spring*, 2000.
- [16] R. Roy and T. Kailath. ESPRIT – estimation of signal parameters via rotational invariance techniques. *IEEE Trans. on Acoustics, Speech, and Signal Processing*, ASSP-37:984–995, July 1989.
- [17] D. Shiu, G. Foschini, M. J. Gans, and J. Kahn. Fading correlation and its effect on the capacity of multi-element antenna systems. *IEEE Trans. Comm.*, 48:502–513, 2000.
- [18] M. Steinbauer, A. F. Molisch, and E. Bonek. The double-directional mobile radio channel. *IEEE Ant. Prop. Mag.*, in press.
- [19] M. Steinbauer, D. Hampicke, G. Sommerkorn, A. Schneider, A. F. Molisch, R. Thoma, and E. Bonek. Array measurement of the double-directional mobile radio channel. In *Proc. IEEE Vehicular Techn. Conf. Spring 2000 - Tokyo*, 2000. IEEE.
- [20] V. Tarokh, A. Naguib, N. Seshadri, and A. R. Calderbank. Space-time codes for high data rate wireless communication: Performance criteria in the presence of channel estimation errors, mobility, and multiple paths. *IEEE Trans. Comm.*, 47:199–207, 1998.
- [21] V. Tarokh, N. Seshadri, and A. R. Calderbank. Space-time codes for high data rate wireless communication: Performance criterion and code construction. *IEEE Trans. Information Theory*, 44:744–765, 1998.
- [22] R. Thoma, D. Hampicke, A. Richter, G. Sommerkorn, A. Schneider, U. Trautwein, and W. Wornitzner. Identification of time-variant directional mobile radio channels. *IEEE Trans. Instrumentation and Measurement*, 49:357–364, 2000.
- [23] J. H. Winters. On the capacity of radio communications systems with diversity in Rayleigh fading environments. *IEEE J. Selected Areas Comm.* 5: 871–878, 1987.